LA-UR- O2 - 6 SS2 .

Title: STUDY OF DISLOCATIONS IN COPPER BY WEAK BEAM, STEREO, AND IN SITU STRAINING TEM:

Author(s): Rodney J McCabe 178257 MST-8
Amit Misra 120292 MST-8
Terence E Mitchell 102631 MST-8

Submitted to: Proceedings of The Mike Meshii Symposium on Electron Microscopy: Its Role in Materials Research. 2003 TMS Annual Meeting. San Diego, CA. March 2-6, 2003

• Los Alamos

NATIONAL LABORATORY

STUDY OF DISLOCATIONS IN COPPER BY WEAK BEAM, STEREO, AND *IN SITU* STRAINING TEM:

Rodney J. McCabe[1]; Amit Misra[1]; Terence E. Mitchell[1]

[1]Los Alamos National Laboratory, MST-8, Struct./Prop. Relations
MS G755, Los Alamos, NM 87545 USA

Abstract

Conventional transmission electron microscopy (TEM) has been an invaluable tool for verifying and developing dislocation theories since the first direct observations of dislocations were made using a TEM in the 1950s. Several useful techniques and technological advancements have been made since, helping further the advancement of dislocation knowledge. The present paper concerns two studies of dislocations in copper made by coupling several of these techniques, specifically weak beam, *in situ* straining, and stereo TEM. Stereo-TEM coupled with *in situ* straining TEM was used for tracking 3D dislocation motion and interactions in low dislocation density copper foils. A mechanism by which dislocations in a pileup bypass a dislocation node is observed and discussed. Weak beam TEM is used in conjunction with stereo-TEM to analyze the dislocation content of a dense dislocation wall (DDW).

3D dynamic observations of dislocations

Individual dislocation interactions are important during all stages of plastic deformation, and can be rate controlling, especially for lower dislocation densities. The present study employs the use of stereomicroscopy in combination with *in situ* straining TEM to study dislocation behavior. The ability to monitor dynamic motion and interactions of dislocations in three dimensions in the TEM would enhance the information obtainable from 2D *in situ* straining and be beneficial for understanding dislocation behavior.

Dislocation nodes and networks are likely important in the deformation and work hardening behavior of fcc metals. They are common in fcc deformation microstructures in dislocation tangles similar to the one observed in this experiment and in dislocation boundaries as discussed in the second half of this paper. A single dislocation with immobile nodes on both ends may act as a dislocation source. Dislocation nodes may also act as barriers to further dislocation motion. If one of the dislocations entering a node is immobile, the node is immobile. Further motion of any of the dislocations in the node might require the coupled motion of the dislocations in the node or unzipping of the node.

Experimental
A 6.35 × 6.35 × 17.7 mm copper (99.995%) compression specimen was annealed at 800°C for 1 hour and furnace cooled. The specimen was then room temperature compressed 1.4 % to add a low density of dislocations. TEM *in situ* tensile specimens were cut, ground, and electropolished from the compression samples with the tensile axis of the TEM specimens corresponding to the compression axis of the compression sample. TEM was performed on a Phillips CM30 at an accelerating voltage of 300 kV.

The stereo-coupled *in situ* experiments involve obtaining 3D descriptions of the dislocation configuration including Burgers vectors prior to and following *in situ* straining in the microscope. The 3D dislocation configurations were obtained using a modified stereo-TEM technique detailed elsewhere [1]. Standard stereomicroscopy of crystalline materials is almost never possible with a single tilt TEM holder making it unfeasible for commercially available *in situ* TEM holders. The modified technique is a weak beam technique involving changing the signs of **g** (the imaging beam) and s_g (the excitation error or how far the imaging beam deviates from the exact Bragg condition) between images while tilting across a Kikuchi band that is at less than approximately 10° to the tilting direction. The experimental error in the third dimension for standard stereo-TEM is around an order of magnitude greater than the measurement error in the other two dimensions and is the same for the modified technique if both **g** and s_g change sign but not magnitude [1]. Quantitative stereo analysis is performed using Sterecon, a 3D reconstruction software [2]. Determination of dislocation Burgers vectors with a single tilt TEM holder is also not generally a straightforward task and often requires standard **g · b** analysis (where **b** is the Burgers vector), dislocation node algebra (Frank's law), and/or image simulation. For the present case all of the analysis was accomplished using **g · b** analysis and dislocation node algebra

Results and Discussion

A stereo pair and corresponding diffraction patterns are shown in Fig. 1 demonstrating the modified stereo technique. The initial 3D configuration is shown in Fig. 2 with the axes corresponding to the stereo coordinate system. In the initial configuration, dislocations 1,2, and 3 are in a pileup against a dislocation wall evident in Fig. 3. The specimen is already under stress at the time the initial structure is measured as is evident by the bowing of dislocations 1-3. These dislocations belong to the slip system with the second largest Schmid factor (0.336), just slightly less than the largest Schmid factor with the tensile axis being [57 69 45]. It is noted that the geometry and stress state in the observed region are fairly complex and the Schmid factors based on a simple tension assumption are approximate.

The interesting aspect of the observed dislocation configuration is that in addition to being in the pile up, dislocation 3 is also pinned at a node with dislocations 6 and 7, all of the
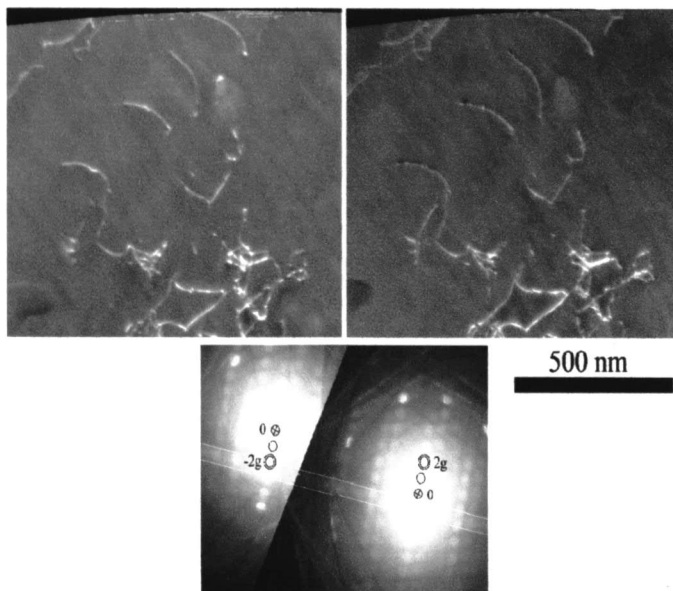
Figure 1. Stereo pair and diffractions patterns using modified stereo technique. In the left image, the −2g spot is used for imaging and the −5g spot is excited (s > 0). In the right image the 2g spot is used for imaging and the −g spot is excited (s < 0). **g** = (111). Tensile axis vertical.
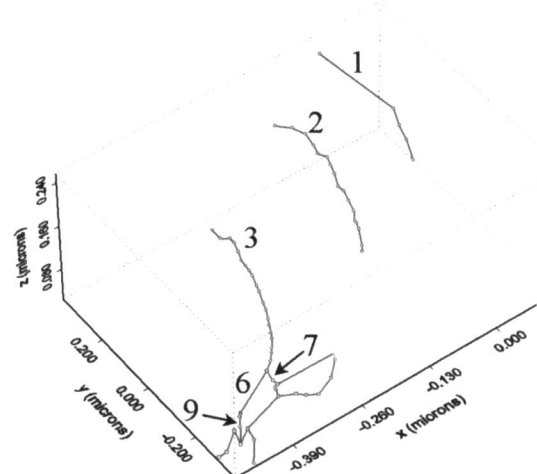

Figure 2. Initial 3D dislocation configuration in stereo coordinate system. The tensile axis is along the y-direction. Dislocations 1 – 5 and 9 have a Burgers vector of [101]; dislocation 6 and 8 have a Burgers vector of [01 $\overline{1}$]; dislocation 7 has a Burgers vector of [110]. Not all dislocations are shown.

dislocations having mixed character. Dislocations 1-3 belong to the ($\bar{1}\,\bar{1}\,1$)[101] slip system. Whether 6 and 7 are on fcc glide planes could not be determined beyond doubt, but it appears dislocation 6 belongs to the (111)[01$\bar{1}$] slip system (Schmid factor of 0.167), and dislocation 7 belongs to the (1$\bar{1}\,\bar{1}$)[110] slip system (Schmid factor of 0.292). Whether or not dislocations 6 and 7 are on slip planes, the dislocation node remains fixed throughout the experiment. Fig. 3 shows the evolution of the dislocation microstructure during *in situ* straining. In Figure 3b, two new dislocations in the pile up sequence (4 and 5) appear and dislocation 4 essentially knocks dislocation 3 off of the node and takes its place at the node. And thus, the pile up advances and the node is bypassed.

From the experiment, it appears that dislocation nodes, at least a single dislocation node in a thin foil, provide minimal resistance to subsequent gliding dislocations on the same slip plane. Unfortunately, it is not possible to see the bypass mechanism occurring during the *in situ* experiment, only the result of the bypass. During *in situ* straining experiments in pure copper, dislocations spend most of the time at pinning points. When the dislocations escape, they move very rapidly between pinning points. Recording at 30 frames per second, it is generally not possible to capture the motion between pinning points.

However, the results of the bypass may be enough to infer what happened during the bypass. During *in situ* straining experiments of copper, gliding dislocations often leave a slip trace on the surfaces of the specimen. There are several important aspects of the slip traces observed for dislocations 3, 4, and 5 in Fig. 3b. First, there is a continuous slip trace on the bottom (right slip trace) surface extending to where dislocation 3 meets the surface. The slip trace on the top surface only extends to where dislocation 4 meets the surface. This would strongly suggest that in the process of bypassing the node, the right side of dislocation 4 combines with dislocation 3 allowing dislocation 3 to escape from the node leaving the left side of dislocation 4 trapped at the node. This bypass is shown schematically in Fig. 4. The applied stress and elastic interactions cause the two dislocations to bow. To a first order approximation, the force between the dislocations is repulsive when the angle between line directions is between -90 and

02:35.83
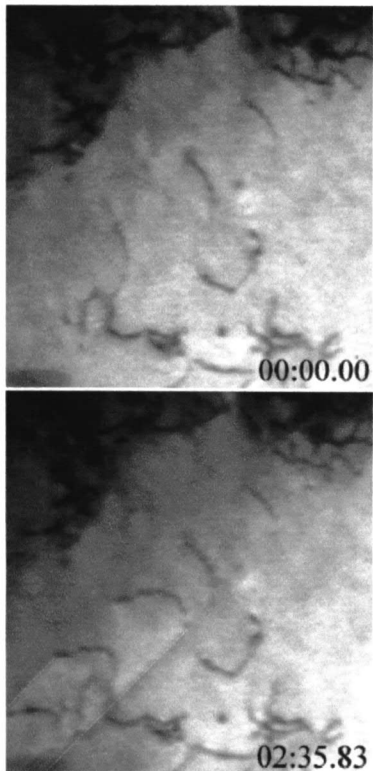
Figure 3. Sequence during *in situ* straining. See text for details
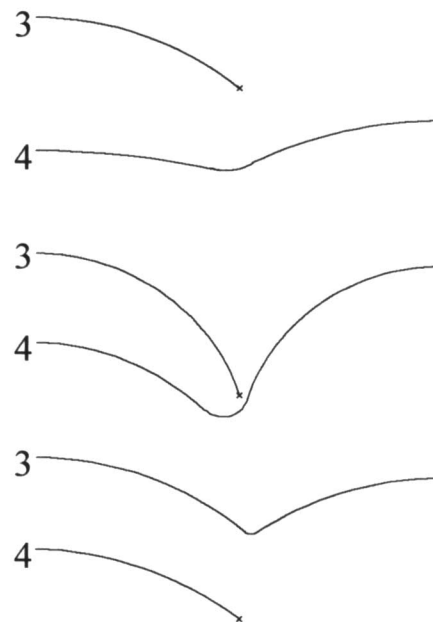
Figure 4. Possible node bypass mechanism. Due to the applied stress and elastic interaction, the dislocations bow until the right side of dislocation 4 is attracted to dislocation 3

+90° and attractive for angles of 90 – 270°. At some point, the force will become attractive between dislocation 1 and the right half of dislocation 2 and these will combine on the other side of the node similar to a Frank – Read source mechanism.

Dense dislocation walls

When medium to high stacking fault FCC metals are deformed (Al, Cu, Ni), cell blocks separated by planar arrays of dense dislocation walls form similar to those shown in Fig. 1. The DDWs characteristically form nearly parallel to the plane(s) of maximum shear stress independent of deformation mode (rolling, tension, torsion, etc.). The misorientation across the DDWs typically increases and spacing decreases with strain. Depending on the crystal orientation (i.e. for crystals oriented for slip on a single slip plane), the DDWs may form close to a {111} plane [3,4].

DDWs are expected to play a significant role in plastic deformation and work hardening behavior, although the exact role is not well understood. Similarly, little is know about the origin and evolution of the dislocation structure of the boundaries. A common assumption is the boundaries are made up of dislocations of the three most active (highest resolved shear stress) slip systems [4,5]. However, this assumption has not been verified experimentally, primarily because of difficulties in imaging individual dislocations in the DDWs. Knowledge of the dislocation content of the boundaries would be valuable for understanding their origin, evolution, and effect on plastic deformation.

There are several factors making the imaging of individual dislocations in DDWs difficult. First, the high dislocation densities associated with DDWs creates problems in imaging individual dislocations. In addition, the crystal orientation changes slightly on either side of each individual dislocation and can change significantly for larger groups of dislocations. This is evident in the difference in diffraction contrast on either side of a boundary, but also in differences within a boundary.

There are several benefits of weak beam microscopy making it better suited to deal with the difficulties of imaging DDW dislocations than two-beam bright or dark field imaging. A primary benefit is the width of the dislocation image is much narrower; thus, the images of individual dislocations have a larger separation. Weak beam is also less susceptible to the difficulties associated with minor changes in orientation. Weak beam imaging is a dark field technique in which the beam used for imaging is not excited (far from the Bragg condition). For non-quantitative weak beam imaging, the range of possible diffraction conditions is reasonably broad. For example, if $g = (111)$ were being used for weak beam imaging, a range of diffraction conditions with excited beams from less than 3g to greater than 6g should result in reasonable contrast for an operating voltage of 300 kV.

Stereo TEM has not been used extensively for studying dislocation structures or behavior. However, stereo TEM can enhance the information obtainable from typical two-dimensional TEM images that are projections of the specimen volume. The advantage of stereo TEM for examining DDWs is it provides additional separation of individual dislocations into the third dimension. This is especially useful when the boundary is composed of more than one set of dislocations (Burgers vectors) as is typical for general low angle boundaries [6].

Results and discussion

The starting material for this experiment was 50.8 × 50.8 × 6.35 mm full hardness copper plate of purity greater than 99.995%. The specimen was vacuum annealed at 700 °C for 2 hours, furnace cooled, and rolled in a single pass to 7.5% reduction. TEM foils were

electropolished from transverse plane sections of the rolled sample. TEM was performed on a Phillips CM30 at an operating voltage of 300 kV.

A single DDW is shown in Fig. 5 for three diffraction conditions. The DDW is orientated within 5° of the $(\bar{1}11)$ plane. Two sets of stereo pairs were obtained, one using a 2g(4g) weak beam condition with $\mathbf{g} = (0\bar{2}0)$, and the second using a g(3g) weak beam condition with $\mathbf{g} = (2\bar{2}0)$. Assuming the DDW are composed of dislocations with $\langle 110 \rangle$ type Burgers vectors, all dislocations should be visible for at least one or both of these diffraction conditions. Numerous dislocation nodes were observed by comparing the two stereo images. The grain containing the DDW is oriented such that the rolling direction is $[81\,\overline{40}\,43]$ and normal direction is $[9\,81\,58]$. The misorientation across the DDWs is 0.46° with an axis of rotation of [13 31 94]. The angle between the DDW plane normal and the axis of rotation is approximately 50° giving the boundary a mixed twist/tilt character. Schmidt factors were obtained assuming perfectly plastic plane strain deformation. Standard Burgers vector analysis was performed using Fig. 5 and other figures not shown with diffraction vectors of (202), $(0\bar{2}\bar{2})$, $(2\bar{2}0)$, $(\bar{1}11)$, and $(00\bar{2})$

The dislocations with the three most common Burgers vectors can be seen in Fig. 5, where **A** marks the same point in all three figures. The most significant observation from the two stereo pairs was the presence of a large number of dislocation nodes. Simplified schematics summarizing the observations from the stereo pairs and $\mathbf{g} \cdot \mathbf{b}$ analysis are shown below the images. Dislocations out of contrast in the images are shown as dotted lines in the schematics. The dislocations visible in both Figs. 5b and 5c at approximately 135° have a line direction of approximately [211] and belong to the slip system $(\bar{1}11)[101]$. This slip system has the second highest Schmid factor of 0.374 and the slip plane is roughly parallel to the plane of the DDW. These dislocations have an average spacing of 85 nm. The dislocations visible in Figs. 5a and 5c at approximately 40° have a line direction of approximately $[01\bar{1}]$ and belong to the slip system (111) $[1\bar{1}0]$. This slip system has the highest Schmid factor of 0.424 with the angle between the slip plane normal and DDW plane normal being approximately 70.5°. These dislocations have an average spacing of 28 nm. The dislocations visible in Fig. 5a at approximately 40° are actually composed of segments of the second set of dislocations with Burgers vectors of $[1\bar{1}0]$ and short segments of dislocations with a Burgers vector of [011]. This can be seen by comparing Figs 5a and 5c, where in Fig. 5c the short segments are out of contrast. This third set appears to also have a line direction of $[01\bar{1}]$ giving them a Lomer dislocation configuration of (100) [011] [7].

The significant presence of dislocations from the two slip systems with the highest resolved shear stresses supports the idea that DDWs form by way of gliding dislocations, as is commonly assumed [4,5]. The presence of the sessile dislocations is very interesting. There is contingent that feels dislocation structures formed during deformation must be low energy structures [8] and the formation of the Lomer dislocations could be a way of further lowering the energy of the DDW [7]. It is certainly likely that the presence of the nodes and Lomer dislocations would make the escape of dislocations in the DDW more difficult.

Conclusions

Some interesting observations have been made about the behavior of dislocations in copper by coupling weak beam, *in situ* straining, and stereo TEM. A mechanism by which dislocations in a pileup bypass a dislocation node and an unforeseen configuration of dislocations in a DDW were observed.
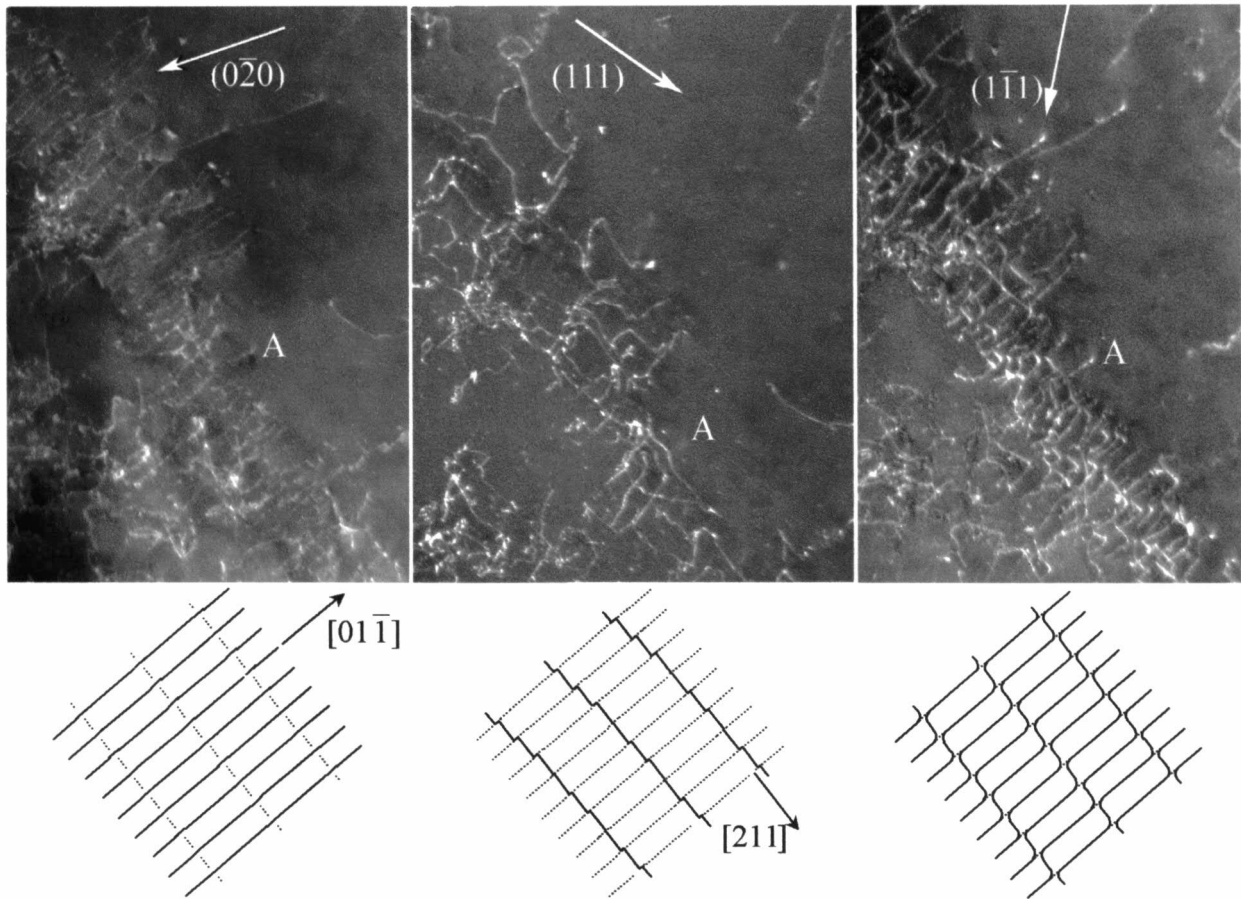
Figure 5. See text for details

References

1. R. J. McCabe, A. Misra, and T. E. Mitchell, "A Single-tilt TEM Stereomicroscopy Technique for Crystalline Materials," Accepted for publication in <u>Microscopy and Microanalysis.</u>

2. M. Marko and A Leith, "Stereocon, Three-Dimensional Reconstruction from Stereoscopic Contouring," <u>J. Structural Biol.</u> 116 (1996), 93-98.

3. Q. Liu and N. Hansen, "Deformation Microstructure and Orientation of F.C.C. Crystals," <u>Phys. Stat. Sol. (a)</u>, 149 (1995), 187-199.

4 . Q. Liu, D. Juul Jensen, and N. Hansen, "Effect of Grain Orientation on Deformation Structure in Cold-rolled Polycrystalline Aluminum," <u>Acta Mater.</u>, 46 (16) (1998), 5819-5838.

5 . J.A. Wert, Q. Liu, and N. Hansen, "Dislocation Boundaries and Active Slip Systems," <u>Acta Metall. Mater.</u>, 43 (11) (1995), 4153-4163.

6 . J.P. Hirth and J. Lothe, <u>Theory of Dislocations</u>, (New York : Wiley, 1982), 697.

7. J. Weertman and J. R. Weertman, <u>Elementary Dislocation Theory</u>, (New York: Oxford University Press, 1992), 93-94

8. D. Kuhlmann-Wilsdorf, "The Theory of Dislocation-based Crystal Plasticity," <u>Phil. Mag. A.</u>, 79 (4) (1999), 955-1008.